Automatic Ribs Segmentation and Counting from Mouse X-ray Images

Omar Al Okashi[1]
Hongbo Du[1]
Joanne Selway[2]
Chris Lelliott[3]
Simon Maguire[3]
Dave Melvin[3]
Sanger Mouse Genetics Project[3]
Kenny Langlands[2]
Hisham Al-Assam*[1]
(hisham.al-assam@buckingham.ac.uk)

[1] Department of Applied Computing, University of Buckingham, MK18 1EG
[2] Buckingham Institute for Translational Medicine, University of Buckingham, MK18 1EG
[3] Wellcome Trust Sanger Institute, Hinxton, Cambridge, CB10 1SA

Abstract

The automatic detection and quantification of skeletal structures has a variety of applications for biological research. This paper proposes an automatic solution for rib segmentation and counting based on structural properties of ribs in mouse X-ray images. The solution consists of five stages, including alignment, cropping the region of interest, image enhancement, rib segmentation, filtering of non-rib objects and rib counting. Experimental results on a set of 100 X-ray images showed consistent good performance of the algorithm compared with a manual annotation by domain experts, with an overall accuracy of about 88%.

1 Introduction

The Mouse Genetics Project [1] was initiated to systematically knock-out mammalian genes and screen for a broad range of resulting traits. One element of the phenotyping pipeline is the thorough evaluation of the skeleton through systematic X-ray imaging of individual animals and manual observations of variation. Given the volume of images that are generated by high-throughput screening, an automated approach to annotation and triaging of images will reduce time and human resource requirements and possibilities of human error.

Accurate identification of any perturbation in skeletal structure is of significant biological relevance. For example, human congenital abnormalities can lead to additional ribs and potential nerve damage to the arms (i.e. thoracic outlet syndrome), whereas loss of ribs can lead to damage within the thoracic cavity due to a lack of protection [2]. Therefore, the identification of genes associated with such abnormalities will provide insight into both specific and generalised abnormalities in skeletal structure.

Our aim is to exploit image processing techniques to enable the automatic counting of ribs from X-ray images of mice. However, this task faces the following specific

challenges. First, the source images in our study are full-body images and hence segmentation of regions of interest (ROIs), i.e. the rib areas, is essential. Second, ribs can be difficult to distinguish in a 2D X-ray image because of their low, sometimes extremely low, colour intensity. Third, most ribs are connected to each other on the edge of the ribcage, making automatic separation a difficult task. Furthermore, the inherent noise in X-ray images presents technical difficulties in rib identification.

Previous work has described rib segmentation and positioning in humans for different medical modalities. The method presented in [3] exploits the capability of Hough Transform to detect lines that determine the first rib in the sagittal plane. The position of the first rib was then used as a reference to determine the initial position of other ribs. Li et al. [4] presented a method that firstly determined the position of the spinal canal after thresholding the image (empirically determined), and then the location for a seed region for every rib. These seeds were then used as a starting point to segment ribs from vertebrae. A model based segmentation was used in [5] to segment and label the ribcage. Triangulated surface models of all 24 ribs were initially created.After that, an adaptation of these models to their corresponding anatomical object to form an initial ribcage was done by using shape constrained model. To determine a proper position for a complete model, a ray based search approach was used to detect a ribs. However, the methods described in [3], [4] and [5] were applied to segment ribs in 3D CT images, and it remains unclear if these methods were applicable to single view X-ray images.

Rib segmentation in X-ray images was considered in [6]. The proposed solution first smooths the image using a Gaussian function, followed by passivation masking, i.e. subtracting the original from the smoothed image. The wavelet image fusion between original and segmented image has been used to enhance the image. After that the Otsu segmentation method [7] has been used to detect lung parenchyma. Finally, ribs were denoised using wavelet and morphology operations such as corrosion and expansion. However, the final result shows connected ribs as well as noises from chest tissues and other organs which makes it unsuitable for automatic counting of the ribs.

This paper proposes a fully-automated method to segment and count ribs in X-ray images. Experimental results on a data set of 100 manually annotated X-ray images confirmed the effectiveness of the proposed method with an overall accuracy of 88%.

2 Proposed Method

Our proposed solution consists of a sequence of 5 steps. The process started with the automatic alignment of a dorsoventral 2D X-ray image to orientate the mouse skeleton in a vertically-upright position. This stage is essential for correct detection of rib ROIs, and to allow later exploitation of left and right ribcage symmetry. After that, a mask image of reference points is used to crop out an ROI containing ribs. This is then followed by image enhancement in spatial and frequency domains to improve the contrast of the cropped area. The next step is the segmentation of ribs from other organs in the chest. The last step is removal of unwanted objects and counting of ribs.

2.1 Automatic Alignment

To perform alignment of the mouse skeleton as shown in Figure 1-a, the spine must be correctly located. We realised that the spine has higher contrast than other surrounding tissues and bone structures. To achieve the objective of spine location, we first applied

adaptive histogram equalization (ADHE) [8] to enhance the contrast, followed by Gamma transformation [9] to highlight the high contrast bones and eliminate other low intensity structures . Morphological operations are then applied to make the spine a complete object without breaks, and to filter out unwanted objects. Once the approximate spine was located, the rotation angle required for the vertical alignment is determined from the bounding box dimensions as illustrated in Figure 1-b using the inverse tangent function. The result of the rotation is shown in Figure 1-c.

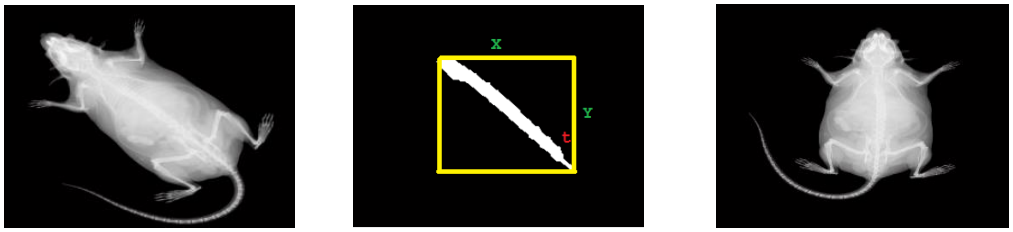

(a) (b) (c)

Figure 1: Alignment process:(a)Input image;(b) Detected spine;(c) Result of alignment.

2.2 Cropping of ROI

To crop the ROI, we need to locate relevant x and y coordinates of the region. It is realised from our observation of the images that such coordinates can be estimated from the x and y coordinates of the limbs. To obtain an image of limbs, we first apply a High Emphasis-Butterworth High Pass Filter (HE-BHPF) [9]. HE-BHPF uses a multiplier to emphasise the high frequency components such as higher contrast bone, limbs and skull while maintaining the low frequency for other organs, as shown in Figure 2-a. This will enable a segmentation of these bones in the next step. After that, the regiongrow segmentation technique that segments different objects by grouping pixel with similar properties (e.g. Intensity) in a region [9] is used to extract high contrast objects such as limbs and skull (shown in Figure 2-b). Once the limbs are segmented, we locate the x and y coordinates of the limbs as shown in figure 2-b, and then use the coordinates to crop the ROI from the original image as shown in figure 2-c.

(a) (b) (c)

Figure 2: Cropping of ROI: (a) Original image processed with the HE-High-Pass filter; (b) Image of processed with region growing segmentation; (c) Cropped ROI.

2.3 ROI Image Enhancement

The cropped ROI may be of very low contrast that may lead to some ribs, particularly the lower ones, being missed by the rib segmentation step. To increase rib contrast, we apply image enhancements through the following two steps:

1. Enhancement in the spatial domain. Similar to the spine location, ADHE is used to enhance the contrast of the overall image first. A median filter is then applied to suppress background noise and smooth the image as shown in Figure 3-a.
2. Enhancement in the frequency domain. It can be seen from Figure 3-a that some overlapping between the ribs and the lung tissues is still present despite the enhancement in spatial domain. For this reason, we decide to further process the enhanced image in the frequency domain by applying first the Butterworth High-Pass filter (BHPF) to highlight and enhances image details, and then a median filter to suppress noise. Figure 3-b shows the result of this step.

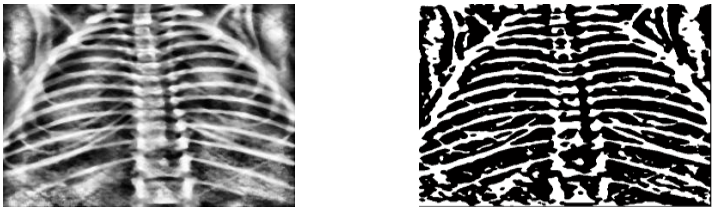

(a) (b)

Figure 3: Enhaning the cropped image: (a) after adaptive HE and median filters, and (b) after applying BHPF and median filters.

2.4 Rib Segmentation

To segment ribs from other structures, we need to remove the spine and the edge of the ribcage from the enhanced ROI. We use the spine outline shown in Figure 1-b as a mask to clear the spine, and split the ROI into two parts as shown in Figure 4-a.

To remove the edge of the ribcage, we proposed a linear function that initiates from the edge of the top rib towards a lower one. This function trims most of the noisy edges of the ribcage and separate the ribs (Figure 4-b). Although crude in cutting off parts of ribs, as we are only concerned with rib counting as opposed to rib length measurement, the function is effective for separating the edge of the ribcage from disjointed ribs.

(a) (b)

Figure 4: Rib Segmentation process: (a) Spine removal ;(b) Ribcage removal and splitting

2.5 Filtering Out Non-Rib Objects and Counting Ribs

It can be seen that the image in Figure 4-b can still not be used directly for rib counting as the image has many non-rib objects that can affect the counting accuracy. By analysing the properties of the ribs, we use the following criteria to remove non-rib objects:

1- Size. If the size of any object is smaller than a specific threshold (i.e. the size of the smallest rib), it will be marked as noise.
2- Shape. Ribs have well-defined shape properties. We approximate each object as shown in Figure 4-b by the smallest ellipse that contains the object, and measure the ratio of

the minor to major axis. Since any rib should have its major axis value greater than its minor axis value, we can eliminate circular, vertical and irregularly-shaped objects.

3- Orientation. After the initial alignment, ribs have expected orientation angles, e.g. a rib cannot be vertical. Therefore, setting a rational threshold for the orientation of left and right ribs can eliminate many non-rib objects.
4- Starting position. All ribs start approximately at the same spatial x-coordinate. Using the mean x-coordinate for the start position of all left and right groups of ribs, non-ribs objects that have start position far away from the mean value, e.g. 2σ, can be removed.

Figure 5 shows the effectiveness of applying these criteria on an example image. Non-rib objects in the circles in Figure 5-a are removed. After filtering, the image is ready for rib counting. This is done by simply scanning along the y-coordinates as shown in Figure 5-c.

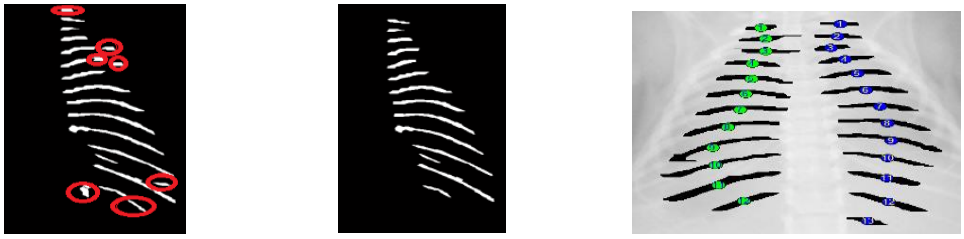

(a) (b) (c)

Figure 5: Filtering-out non rib objects: (a) Before filtering, with non-ribs circled; (b) Filtering using rib properties; (c) Final annotated image.

3 Experiments and Discussion

We have tested our method on a dataset of 100 full body dorsoventral view X-ray images that were previously manually annotated by domain experts. These 100 images include a variety of images of different degrees of difficulties in image analysis. Since the proposed solution goes through three main stages, i.e. body alignment, ROI cropping, and rib segmentation and counting, we evaluate the accuracy at each of the three stages separately. Automatic body alignment is considered accurate if the position of the body is in a vertical position by observation.The results show that our automatic alignment achieves an accuracy of 98%. The ROI cropping is considered accurate if the cropped area isolates all the ribs without missing any. Our method cropped 98 out of 98 correctly aligned images, i.e. 100% accuracy. The two inaccurately aligned images has caused error at the cropping stage where the top rib is not included in the area as shown in Figure 6-a.

(a) (b)

Figure 6: Examples of inaccurate counting: (a) Missed upper (b) Merged ribs.

Out of the 98 images that were correctly cropped, ribs in 86 of them (i.e. 87.8%) were counted accurately according to the manual annotations. The other 12.2% of images

contain missing, merged or discontinuous ribs. Missing ribs occur due to extremely low intensity of lower ribs, or errors in removing ribcage edges. Merged ribs, as shown in Figure 6-b, can be a result of reflection due to the noisy nature of X-ray images.

4 Conclusions

Segmentation and counting of ribs is essential for assessing skeletal phenotype. We proposed a fully-automated algorithm that segments and counts ribs in X-ray images. We have demonstrated a comparable accuracy with existing manual methods, and shown the ability of our solution to overcome a variety of challenges presented by the segmentation of X-ray images. The aim of this study was to locate and count ribs rather than to segment and identify them in their entirety.We are now working to improve the level of accuracy of the alignment, and the removal of non-rib objects by exploiting more sophisticated filters and investigating various thresholds used in this process. Our future work also includes a more in-depth analysis for the proposed schemes on a larger set of images.

5 Acknoweledgment

We thank the Sanger Research Support Facility, ES Cell Mutagenesis, Transgenic Technologies and Mouse Informatics Groups for support in providing the mice, X-Rays and images used in this paper.

6 References

[1] J. White,G. Anna-Karin, N. Karp, E. Ryder, M. Buljan, J. Bussell, J. Salisbury, S. Clare, NJ. Ingham , C.Podrini, R .Houghton , J.Estabel, JR.Bottomley, D.Melvin,D.Sunter ,N.Adams; D.Tannahill, D .Logan, D .Macarthur, J.Flint , V.Mahajan, SH.Tsang ,I. Smyth, F.Watt , W.Skarnes , G.Dougan , D.Adams , R.Ramirez-Solis ,A.Bradley , KP .Steel . Genome-wide generation and systematic phenotyping of knockout mice reveals new roles for many genes. Cell 154, no. 2, pp. 452-464, 2013.

[2] D. Wattanasirichaigoon, C. Prasad, G. Schneider , J. A. Evans and B. R. Korf, Rib defects in patterns of multiple malformations: a retrospective review and phenotypic analysis of 47 cases, *American Journal of Medical Genetics Part A*, vol. 122, no. 1, pp. 63-69, 2003.

[3] H.Li, J.Li, S. Guo, J. Liu, and Y. Kang. Automatic rib positioning method in CT images. *In Bioinformatics and Biomedical Engineering (iCBBE), 2010 4th International Conference* , pp. 1-4. IEEE, 2010.

[4] J. Lee and A. Reeves. Segmentation of individual ribs from low-dose chest CT. *In SPIE Medical Imaging*, pp. 76243J-76243J. International Society for Optics and Photonics, 2010.

[5] T. Klinder, C. Lorenz, J.Berg, S. Dries, T. Bülow, and J. Ostermann. Automated model-based rib cage segmentation and labeling in CT images. *In Medical Image Computing and Computer-Assisted Intervention*–MICCAI 2007, pp. 195-202. Springer Berlin Heidelberg, 2007.

[6] W. Cui; T.Yu; L.Ren; H.Shao, Ribs segmentation based on image fusion and wavelet de-noising, *Biomedical Engineering and Informatics (BMEI), 2012 5th International Conference on* , vol., no., pp.362,366, 16-18 Oct. 2012.

[7] N.Otsu, A Threshold Selection Method from Gray-Level Histograms, *IEEE Transactions on Systems*, Man, and Cybernetics, Vol. 9, No.1, pp. 62-66, 1979.

[8] W. Pratt, Digital Image Processing, 3rd ed., Wiley, 2001.

[9] R. Gonzalez and R.Woods, Digital Image Processing, 3rd ed., Pearson International Edition, 2008.